International Journal of Computer Information Systems and Industrial Management Applications
ISSN 2150-7988 Volume 18(4s) 2026 pp. 1121-1138
https://doi.org/10.70917/ijcisim-2026-xxxx
Article

Memory-Aware Quasi-Cyclic Spatially Coupled LDPC Code Design for DVB-S2X Satellite Communication Systems over AWGN Channels

Sandip J. Dawda[1], Saurabh Mehta[2]

[1]Department of Electronics and Communication Engineering, Government Engineering College, Sector-28, Gandhinagar, Gujarat, India.
Email: sandip_dawda@gecg28.ac.in
[2]Department of Electronics and Telecommunication Engineering, Vidyalankar Institute of Technology, Vidyalankar Campus, Vidyalankar College Marg, Wadala (East), Mumbai, Maharashtra, India.
Email: saurabh.n.mehta@gmail.com; sau.mehta@yahoo.co.in

Abstract: Satellite communication systems are essential for global connectivity but are constrained by long propagation delays, channel impairments, and severe noise, particularly in low-SNR environments. Reliable data transmission therefore demands highly robust forward error correction techniques. Although DVB-S2X LDPC codes are widely used, they still exhibit limitations in short-cycle suppression, structural optimization, and hardware efficiency in practical deployments. This study proposes a memory-aware QC-SC-LDPC code design for satellite communication over AWGN channels. The proposed scheme involves the combination of deterministic spatial coupling, adaptive irregular protograph generation, pairwise cycle-aware PEG algorithm for optimization, and QC-lifting process. The use of memory-based banded coupling scheme is employed in order to increase local connectedness, minimize harmful short cycles, and enable faster decoding convergence along with high implementation efficiency. Numerical simulation analysis carried out using the DVB-S2X short frame parameters reveals that the proposed scheme outperforms classical LDPC codes. For the QPSK 32/45 case, a coding gain of 0.36 dB is achieved at the desired FER, whereas for the QPSK 11/45 case, coding gains of 4.25 dB under E_s/N_0 and 2.86 dB under E_b/N_0 are realized, showing high resiliency even under very low SNR conditions. The result clearly shows that there is significant improvement in waterfall characteristics and error-floor performance. The proposed QC-SC-LDPC framework provides a scalable and hardware-efficient solution for reliable satellite communication systems, with potential extensions toward fading channels, non-terrestrial networks, and real-time hardware deployment.
Keywords: QC-SC-LDPC codes, DVB-S2X, Satellite Communication, AWGN Channel, Spatial Coupling, Quasi-Cyclic LDPC, Progressive Edge-Growth (PEG), Tanner Graph.

1 Introduction

Satellite communication is seen as an important technology for the next generation of wireless communication systems because it has the advantages of broad coverage and high data rates, which make up for the problems with ground relay systems. These qualities enhance terrestrial communication infrastructures, especially in areas where ground relay systems are constrained or impractical [1],[2]. According to [3], the global satellite market is projected to grow nearly sevenfold, from the current 15 billion to $108 billion by 2035. This rapid expansion is expected to deliver high-speed, low-latency, and ubiquitous internet and communication services worldwide.

At the physical layer, Digital Video Broadcasting – Satellite, Second Generation (DVB-S2) and its expansion DVB-S2X are two of the most extensively used standards, offering significant performance improvements over earlier systems [4]. However, satellite communication systems have problems that come with the technology, like long propagation delays, especially in geostationary orbits where the round-trip delay is about 240 to 279 ms. There are also channel impairments caused by changes in elevation angles and weather conditions [5] [6].

To ensure reliable satellite communication under such conditions, robust forward error correction (FEC) solutions are required to cope with noisy channels and keep data secure. Some of the common types of convolutional FEC algorithms include turbo product codes (TPCs), convolutional codes, and Reed–Solomon (RS) codes [7]. Efficient coding and decoding algorithms greatly minimize the signal-to-noise ratio (SNR) needed for a certain bit error rate (BER) in satellite communication systems. This makes it possible to use less power for transmission and build smaller hardware [8]. Low-density parity-check (LDPC) codes, especially quasi-cyclic LDPC (QC-LDPC) codes, have become more popular because they are better at correcting errors and use less hardware. QC-LDPC codes exploit structural regularity in the parity-check matrix, reducing memory and interconnect complexity while achieving near-optimal performance [9]. Efforts have been expended in order to make them suitable for wireless communications [10], [11], as LDPC block codes are known to approach channel capacity [12].

Further advancements in coding theory have led to the development of spatially coupled LDPC (SC-LDPC) codes have been shown able to achieve the channel capacity under belief propagation-based iterative decoding, for a wide range of channels, owing to the convolutional structure of their parity-check matrix, which triggers the well-known threshold saturation phenomenon [13],[14].

The performance of such iterative decoders, however, is significantly affected by the code representation, in addition to its structural properties. In fact, iterative decoding is performed on a bipartite graph known as Tanner graph [15], which has a small number of edges corresponding to the small number of ones in the sparse parity check matrix of an LDPC code. In particular, short cycles in the graph reduce the independence of exchanged messages, thereby degrading decoding performance. Furthermore, harmful structures such as trapping sets and absorbing sets are known to dominate the error-floor behavior over Additive White Gaussian Noise (AWGN) channels

[16],[17]. These structures are often closely associated with cycles and their combinations, and their presence leads to notable degradation in error-correction capability [18].

In terms of decoding, the sum-product (SP) algorithm, also known as belief propagation (BP), remains the performance benchmark for LDPC decoding [19], but its probability-domain arithmetic is computationally expensive for resource-constrained field-programmable gate arrays (FPGA). Simplified variants such as min-sum (MS) [20],[21] and normalized min-sum (NMS) reduce complexity by replacing multiplications with add-compare-select operations, albeit at the cost of some coding gain.

To mitigate these impacts, two main solutions are usually used: optimizing the code architecture to minimize hazardous structures [18],[22], and upgrading decoding algorithms to make them more resistant [23]. Among them, design-based techniques are often chosen because they are more flexible and better at managing graph features throughout development [24]. When it comes to SC-LDPC codes, a popular way to build them is to use edge-spreading methods to turn LDPC block codes into linked structures [24]. However, the performance of the resulting SC-LDPC codes remains dependent on the quality of the underlying base graph and the adopted spreading strategy.

To combine the best features of SC-LDPC codes with QC-LDPC structures, quasi-cyclic spatially coupled LDPC (QC-SC-LDPC) codes have been developed as an efficient hybrid solution. Recent research indicates that QC-SC-LDPC codes using compact base graphs attain decoding performance akin to traditional LDPC codes in broadcasting contexts, eliminating the need for intricate bit-mapping modification [25]. With implementation-oriented sliding window decoding algorithms [26], they can attain similar decoding complexity while preserving the advantages of spatial coupling, and their near-regular row degree distributions enable high-throughput implementations using low-precision quantized decoding techniques [27]. For quasi-cyclic realizations, QC-SC-LDPC codes are typically constructed using protographs, which provide a compact representation of the Tanner graph, where the design of the spreading matrix critically influences girth, cycle distribution, and the presence of harmful substructures. Consequently,

protograph-based constructions have demonstrated strong asymptotic and finite-length performance across various communication scenarios [28],[29].

Motivated by these observations, this study proposes a memory-aware QC-SC-LDPC code design framework that combines structured protograph building with progressive edge-growth (PEG)-based shift optimization for DVB-S2X systems over AWGN channels. The proposed framework integrates quasi-cyclic and spatially connected designs into a single architecture, which is different from traditional methods that tackle them individually. In order to meet the highly reliable transmission requirements of satellite communication systems, the proposed approach introduces a deterministic, memory-controlled banded spatial coupling mechanism is introduced, preserving locality while enhancing connectivity, thereby improving decoding convergence and mitigating error-floor effects. Additionally, the framework incorporates rate-adaptive irregular column degree distributions to achieve better threshold performance and the PEG algorithm is employed during quasi-cyclic lifting to optimize shift assignments, thereby maximizing girth and eliminating short cycles in the Tanner graph. This unified design enables a practical, scalable, and hardware-efficient QC-SC-LDPC construction while maintaining compatibility with DVB-S2X requirements, and its effectiveness is validated through FER and BER performance comparisons against standard DVB-S2X LDPC codes.

The main contributions of this study are summarized as follows:

- A novel QC-SC-LDPC protograph construction method is proposed, incorporating a banded spatial coupling mechanism with controllable memory to improve decoding performance and structural regularity.
- The study introduces an adaptive column degree distribution strategy that enhances convergence behavior and reduces error floors, particularly for high-rate codes.
- A scalable quasi-cyclic lifting approach is developed, enabling efficient generation of large parity-check matrices suitable for practical implementation.
- The proposed QC-SC-LDPC codes are evaluated over AWGN channels using iterative decoding, and their performance is compared with DVB-S2X LDPC benchmarks in terms of frame error rate (FER) and BER.
- A robust MATLAB-based simulation environment is developed, supporting multiple decoding algorithms (e.g., layered belief propagation, min-sum variants) and adaptive stopping criteria.

2 Literature Review

LDPC codes have the performance of approaching the Shannon limit [30], high coding gain, and strong anti-interference ability [31]. These have now become a part of the channel code standard recommended by the Consultative Committee for Space Data Systems (CCSDS). Many studies have been done in the area of enhancing their decoding speed, hardware implementations, and reliability on real channels. This section summarizes key developments in this domain.

LDPC codes feature a low decoding threshold, a straightforward coding structure, and ease of hardware implementation when compared to conventional RS codes and convolutional codes [32]. LDPC codes are better appropriate for parallel high-throughput encoder–decoder architecture because they have less coding complexity than Turbo codes. [33]. LDPC codes have flexible bit-rate structures [34] and low error levels [35] and meet the application scenario of satellite link communication, so they have been widely used in the field of satellite communications [36]. For instance, Vassallo et al. [37] presented a novel early termination stopping criterion for LDPC decoders that is based on detecting the periodicity of syndrome weight oscillations. This design can reduce computational energy and can be implemented to meet the energy resources of satellite communications. Gumede et al. [38] presented filtered orthogonal frequency division multiplexed LDPC codes, which can achieve a coding gain of 1.2 dB with a BER of under moderate rain weather conditions and can be well applied to Ka-band satellite communications. The study by [34] proposed an efficient multi-rate QC-LDPC code construction technique which is applicable to satellite communication systems and which outperforms DVB-S2X LDPC codes in terms of performance at all code rates.

Recent studies on LDPC-based satellite communication systems [39],[40],[41],[42],[43],[44] emphasized the development of efficient decoding algorithms, hardware realization, improved error performance, and reliable system operation under realistic channel environments. The topics of interest include optimal decoder designs, low-complexity iterative decoding schemes, multirate QC-LDPC coding, synchronization issues, and SC-LDPC construction methods. A summary comparison of these studies is shown in Table 1 below.

Table 1 Summary of Recent Advances in LDPC-Based Satellite Communication Systems

Ref.	**Approach**	**Key Contribution**	**Application**	**Performance Insight**	**Limitation**
[39]	LDPC decoder architecture	Efficient check-node design + non-uniform quantization	Satellite communication systems	~76.5 Gbps throughput	High hardware complexity under large-scale deployment
[40]	3D product code decoding	Reduced-complexity iterative decoding	Satellite links	0.15–0.3 dB gain	Limited scalability for long code lengths
[41]	SC-LDPC circulant design	Flexible SC-LDPC construction	Satellite + 6G	>0.5 dB gain over SC-5G-LDPC at BER 10^{-6}; ~50% lower decoding complexity vs SWD	High memory usage in practical hardware
[42]	LDPC decoding optimization	Reliability-enhanced iterative decoding	Satellite systems	~0.4 dB gain, fewer iterations	Performance depends on channel conditions (AWGN only)
[43]	Layered QC-LDPC decoder	Parallel scheduling architecture	5G/NTN	Up to 2.85× throughput improvement with reduced loss	Pipeline conflicts still partially persist

				(0.6 dB → 0.2 dB).	
[44]	External synchronizati on (DVB)	Doppler-aware synchronization	GEO satellites	Improved BER & SNR stability	Not integrated with channel coding optimization

Despite considerable progress in LDPC-based satellite communication systems, there are still certain problems that need to be resolved. Most of the research that have been done so far concentrate on single enhancements, including optimizing the architecture of decoders, making iterative decoding less complicated, building spatially linked LDPCs, designing multi-rate QC-LDPCs, and synchronization enhancement. However, these approaches typically optimize LDPC structure, decoding, or synchronization in isolation, resulting in fragmented design strategies that do not fully exploit joint graph-structural and hardware-aware optimization for practical DVB-S2X systems. Furthermore, although QC-LDPC and SC-LDPC structures both provide robust error-correction functionalities, their combined architecture with regulated memory, enhanced girth, and organized quasi-cyclic spatial coupling has yet to be thoroughly investigated. Also, a lot of current approaches have problems with large memory needs, leftover pipeline inefficiencies, limited capacity to respond to changes in rate, and no structural optimization for short-cycle mitigation. Consequently, there is a clear necessity for a single, memory-efficient QC-SC-LDPC framework that improves decoding efficiency, lowers error levels, and makes sure that DVB-S2X satellite communication systems can function with more hardware under AWGN channels.

3 Methodology

This study proposes a memory-aware QC-SC-LDPC code design methodology for robust satellite DVB-S2X systems on AWGN channels. The suggested design approach integrates deterministic spatial coupling, adaptive irregular protograph design, cycle-aware PEG-based edge placement, QC shift determination, and QC structured lifting in a single coding framework. The major focus of the work is on enhancing the decoder's convergence capability by reducing the effects of problematic short cycles and trapping sets in the corresponding Tanner graph. At the same time, high performance and hardware efficiency should be preserved. Unlike classical LDPC block codes, the suggested design approach incorporates deterministic memory-based banded spatial coupling with an adaptive irregular degree distribution pattern, cycle-aware PEG-based optimization, and quasi-cyclic shift placement into a unified construction algorithm. The novelty of the suggested approach is the integration of all mentioned features into one consistent construction paradigm.

The proposed framework comprises six essential components, which include (i) spatially coupled protograph construction considering memory effect, (ii) adaptive irregular degree-distribution setting, (iii) pairwise cycle-aware edge positioning through PEG algorithm, (iv) quasi-cyclic shifts using PEG algorithm, (v) lifting of quasi-cyclic graph with parity check matrix creation, and (vi) iterative decoding along with its performance evaluation under AWGN channels. These components altogether help in the design of optimized and hardware-friendly QC-SC-LDPC code for DVB-S2X satellites. Figure 1 illustrates the overall workflow of the proposed QC-SC-LDPC design framework.

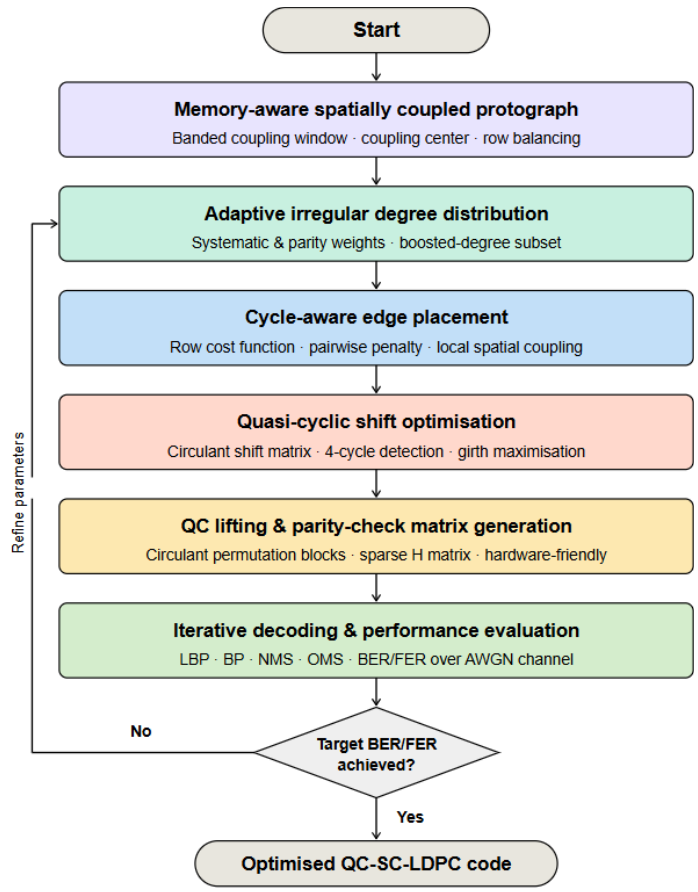

Figure 1 Flowchart of the proposed memory-aware QC-SC-LDPC code design framework

3.1 System Model

The satellite communication system considered in this study analysis conforms to the DVB-S2X short frame transmission model on an AWGN channel. The Binary phase-shift keying (BPSK) modulation scheme has been adopted due to its resilience, simplicity in implementation, and applicability in satellite communication channels experiencing noisy environments.

Let the transmitted coded bit sequence be transformed to a bipolar BPSK signal sequence given by

$$x_i \in \{+1, -1\}, i = 1,2, \dots, N \qquad (1)$$

where N is the length of the transmitted codeword. From Eq. (1), it is clear that each coded bit is transformed into either +1or -1 before being sent across the satellite channel.

The transmitted sequence is then passed over an AWGN channel, and the received sequence can be expressed as

$$y_i = x_i + n_i \qquad (2)$$

where y_i is the received signal that corresponds to the transmission of x_i, and n_i represents the noise term added in the Gaussian channel. Eq. (2) explains the effect of channel noise on the transmission of BPSK symbols through satellite communication.

The noise samples are assumed to be independent and identically distributed Gaussian random variables with zero mean and variance σ^2, which is represented as

$$n_i \sim \mathcal{N}(0, \sigma^2) \qquad (3)$$

As defined in Eq. (3), the AWGN channel adds independent Gaussian noise samples to the input signal sequence.

At the receiver end, decoding of the received bits is done using soft decision decoding based on the log-likelihood ratios of the received channel observation. The channel LLR of the i^{th} received bit when transmitted through the AWGN channel using BPSK modulation is given by

$$L(y_i) = \frac{2y_i}{\sigma^2} \qquad (4)$$

where $L(y_i)$denotes the reliability information associated with the received symbol y_i. From Eq. (4), it can be seen that the higher the value of positive and negative log-likelihood ratio magnitudes,the more confidence there is about determining whether +1 and -1 are transmitted, respectively. The computed LLR values are subsequently utilized as input messages for the iterative QC-SC-LDPC decoding process operating on the Tanner graph representation of the proposed code structure. The decoding is an iterative exchange of messages between variable nodes and check nodes until the symbols become more reliable and recover the transmitted information sequence.

3.2 Memory-Aware Spatially Coupled Protograph Construction

The QC-SC-LDPC code is initially designed based on the following sparse binary protograph matrix expressed by

$$B_{SC} \in \{0,1\}^{M_b \times N_b} \qquad (5)$$

where M_b and N_b denote the numbers of check-node groups and variable-node groups, respectively. As shown in Eq. (5), the protograph matrix acts as the simplified base graph before quasi-cyclic lifting.

While typical LDPC block codes are built in a stochastic fashion, the proposed framework utilizes a deterministic spatial coupling structure that takes memory into account. In particular, each column in the variable node will only be coupled to a limited number of rows from the check node in a specific spatial coupling region.

For a variable-node index j, the admissible coupling window is defined as

$$W(j) = [\max(1, j - w), \min(M_b, j + w)] \qquad (6)$$

where w is the parameter that defines the bandwidth of coupling memory. As shown in Eq. (6), parameter w defines the range of possible connections between check nodes, resulting in a structured banded coupling pattern.

To further preserve spatial locality, the coupling center associated with each variable-node column is deterministically assigned according to

$$r_c(j) = 1 + \frac{(M_b - 1)(j - 1)}{N_b - 1} \qquad (7)$$

where $r_c(j)$ represents the row index associated with the j^{th} variable node group. This equation disperses the coupling centers incrementally in the protograph framework, yielding a diagonally band-limited Tanner graph topology.

The local coupling mechanism specified in Eq. (6) and Eq. (7) greatly enhances iterative message passing performance without imposing overly redundant graph connections. The resulting design offers better routing performance, maintains structural regularity, and boosts hardware scalability for extended DVB-S2X frames.

The sparsity density of the protograph matrix is represented as

$$\rho = \frac{\text{nnz}(B_{SC})}{M_b N_b} \qquad (8)$$

where nnz(·) denotes the number of nonzero elements in the protograph matrix. As expressed in Eq. (8), the sparsity ratio controls the graph connection density which affects both decoding complexity and message-passing efficiency.

The framework uses localized coupling together with row-balancing operations to prevent the occurrence of isolated low-degree check nodes and weak structural graph areas which create obstacles for decoding stability and generate trapping sets and short cycles. The balancing process improves graph uniformity while it strengthens the capacity of iterative decoding to perform better.

3.3 Adaptive Irregular Degree Distribution

In order to enhance decoding threshold and iterative behavior, the introduced scheme makes use of adaptive irregular variable-node degree profiles. Various weights for systematic and parity parts of the protograph are considered for the specific target code rate of the DVB-S2X coding scheme.

In case of low-rate coding schemes, high variable-node degrees are used to optimize the decoding threshold and increase the capacity of correcting errors. On the other hand, in high-rate coding systems, deliberate irregularity is applied to minimize graph density without compromising decoding thresholds and minimizing harmful degree-2 variable-node structures that adversely affect the waterfall region.

Let $d_v(j)$ denote the degree of the j^{th} variable node. The proposed degree assignment strategy is defined as

$$d_v(j) = \begin{cases} d_{\text{sys}}, & j \in S \\ d_{\text{par}}, & j \in P \end{cases} \qquad (9)$$

where S represents the set of systematic variable nodes and Prepresents the set of parity variable nodes, while d_{sys} and d_{par} denote the corresponding column weights assigned to the systematic and parity sections, respectively.

As defined in Eq. (9), different degree profiles are assigned to systematic and parity regions in order to achieve improved decoding convergence and balanced graph connectivity.

To further enhance waterfall-region decoding performance, the proposed framework introduces controlled irregularity by assigning boosted degrees to selected variable-node subsets. The boosted-degree assignment is represented as

$$d_v^{\text{boost}}(j) = d_v(j) + 1 \qquad (10)$$

For selected variable-node groups, Eq. (10) assigns one additional edge connection to improve graph expansion properties and iterative decoding reliability. Subsequently, row degrees are balanced to ensure uniform check-node participation and to reduce the probability of harmful trapping structures.

3.4 Pairwise Cycle-Aware PEG Edge Placement

After the target variable-node degree distributions have been established, the proposed framework uses PEG-based localized edge placement to create the spatially coupled protograph while it works to minimize local cycle formation. The edge-placement strategy handles three main tasks which include maintaining row balance and keeping local spatial connections intact while preventing multiple row connections from being established during the graph construction.

For each candidate row connection, a row-selection cost function is evaluated as

$$C(r) = \alpha D_r + \beta \mid r - r_c \mid + \gamma P_r \qquad (11)$$

where D_r denoting the current degree of the row, r_c representing the coupling-center row, and P_r representing the penalty for pair-wise cycles. The values of the parameters α, β, and γ can be adjusted by choosing appropriate weights, where it is guaranteed that $\alpha + \beta + \gamma = 1$. In general, larger values of α indicate greater importance for degree balancing, larger values of β denote greater importance for locality preservation, and larger γ values imply greater preference for avoiding short-cycles

According to Equation (11) the cost function developed by the authors shows preference to candidate rows which exhibit better connectivity and shorter coupling distances and fewer instances of repeated row-pair use. The framework can maintain localized coupling functions which work to decrease the chances of creating harmful cycle patterns.

The pairwise cycle penalty is computed using the occurrence matrix that records repeated occurrences of row-pair interactions in constructing the protograph. Given two rows, r_1 and r_2, the pairwise penalty is defined by

$$P(r_1, r_2) = N_{\text{pair}}(r_1, r_2) \qquad (12)$$

where $N_{\text{pair}}(r_1, r_2)$ denotes the number of previously established shared connections between the row pair (r_1, r_2). From Eq. (12), it can be seen that higher values of penalty translate into higher probabilities of interaction between row pairs that could result in short-cycles being formed in the Tanner graph.

The edge-selection process involves selecting row pairs with minimal costs iteratively with the aim of optimizing row interconnections, sustaining local spatial coupling, avoiding repeated row pair formations, and minimizing the probability of short cycles being created The proposed pairwise cycle-aware PEG mechanism helps to improve Tanner graph expansion properties of the system while reducing the decoding error-floor degradation problems which arise from trapping structures.

3.5 PEG-Based Quasi-Cyclic Shift Optimization

After the pairwise edge placement considering cycles, the second part of the proposed algorithm involves quasi-cyclic lifting through circulant permutation matrices of dimensions $Z \times Z$, where Z represents the lifting parameter. The lifting process transforms the compact protograph into a massive sparse parity-check matrix while maintaining its structural regularity and implementation efficiency.

A circulant shift matrix is generated as

$$S \in \{-1, 0, 1, \ldots, Z-1\}^{M_b \times N_b} \qquad (13)$$

where each non-zero entry corresponds to the circulant shift induced by a non-zero link in the protograph, and −1 represents the lack of such a link. The shift matrix specifies the cyclic permutation operation to be performed on each circulant block during lifting using the definition provided in Eq. (13).

In order to achieve the maximum girth of a graph and avoid undesirable short cycles, the approach utilizes a PEG optimization algorithm for circulant shift assignment. The optimization procedure iteratively selects shift values that minimize local cycle formation and improve Tanner graph expansion characteristics.

For any two rows i_1 and i_2 sharing columns j_1 and j_2, a 4-cycle exists if

$$(s_{i_1,j_1} - s_{i_1,j_2} + s_{i_2,j_2} - s_{i_2,j_1}) \bmod Z = 0 \qquad (14)$$

where $s_{i,j}$ represents the circulant shift value for the respective protograph entry. Equation (14) shows that a zero modular difference implies the presence of a detrimental 4-cycle in the Tanner graph lift. The design process ensures that these situations do not occur to optimize the minimum girth value and avoid detrimental cycle structures that lead to poor decoding performance.

3.6 **Quasi-Cyclic Lifting and Parity-Check Matrix Generation**

Utilizing the optimal shift values for the circulant shifts determined in the earlier stage, the complete parity check matrix is constructed via quasi cyclic lifting. This involves substitution of all nonzero entries in the protograph matrix with the circulant permutation matrix with the specified shift value.

The resulting parity-check matrix is represented as

$$H_{QC} = \begin{bmatrix} P_{s_{1,1}} & P_{s_{1,2}} & \cdots & P_{s_{1,N_b}} \\ P_{s_{2,1}} & P_{s_{2,2}} & \cdots & P_{s_{2,N_b}} \\ \vdots & \vdots & \ddots & \vdots \\ P_{s_{M_b,1}} & P_{s_{M_b,2}} & \cdots & P_{s_{M_b,N_b}} \end{bmatrix} \qquad (15)$$

where $P_{s_{i,j}}$ denotes a $Z \times Z$ circulant permutation matrix shifted by $s_{i,j}$. The lifting process, as per Eq. (15), converts the small-sized graph form to a large-sized parity-check matrix that can be used for practical coding and decoding operations.

The quasi-cyclic structure needs less memory for its encoder and decoder functions because it requires only the storage of circulant shift values instead of the complete parity-check matrix. The regular circulant arrangement allows for parallel hardware implementation which uses efficient routing systems and scales better with larger DVB-S2X frame lengths.

3.7 Iterative Decoding Algorithm

The decoding process for QC-SC-LDPC codes uses iterative message-passing algorithms which operate on the Tanner graph representation of the lifted parity-check matrix. The primary decoding algorithm employed in this study is layered belief propagation (LBP), owing to its faster convergence behavior and lower decoding latency compared with conventional flooding-based scheduling approaches.

In the min-sum approximation, the check-node update operation is expressed as

$$L_{c\to v} = \left(\prod_{v' \in N(c)\setminus v} \operatorname{sign}(L_{v'\to c}) \right) \min_{v' \in N(c)\setminus v} | L_{v'\to c} | \qquad (16)$$

where $L_{c\to v}$ denotes the message passed from check node c to variable node v, and $N(c)$ indicates the set of adjacent variable nodes connected to check node c. As per Eq. (16), the check node message is calculated using the multiplication of the signs of messages received from adjacent nodes and the minimum absolute value of all incoming messages.

The variable-node update operation is computed as

$$L_{v\to c} = L_{ch,v} + \sum_{c' \in N(v)\setminus c} L_{c'\to v} \qquad (17)$$

where $L_{ch,v}$ stands for the channel log-likelihood ratio (LLR) associated with variable node v, and

$N(v)$ is the set of neighboring check nodes that connect to the variable node v. Eq. (17) shows how the variable node message is updated based on the reliability of the channel information and the incoming messages from the check nodes. The decoding process continues until all parity-check constraints have been checked or until the system reaches its maximum decoding iteration limit. The simulation framework evaluates decoding performance through multiple decoding variants which include layered belief propagation together with belief propagation (BP) and normalized min-sum (NMS) and offset min-sum (OMS) decoding methods to assess how different operational conditions affect system performance and decoding speed and implementation efficiency.

3.8 Performance Evaluation

The effectiveness of the proposed QC-SC-LDPC system is analyzed through extensive simulations based on the AWGN channel using DVB-S2X short frame configurations. The simulation analysis is mainly concentrated on decoding performance, convergence behavior, and graph structure performance when subjected to iterative decoding.

Performance criteria for the proposed code schemes include BER (bit error rate), FER (frame error rate), decoding convergence properties, lower bound of the girth parameter, decoder speed, and sparsity property of the code structure. Among these performance measures, BER and FER can be viewed as the key error-correcting and decoding performance measures.

The frame error rate is computed as

$$FER = \frac{N_f^{err}}{N_f} \quad (18)$$

where N_f^{err} stands for the total number of faulty frames and N_f is the total number of transmitted frames.

Similarly, the bit error rate is calculated as

$$BER = \frac{N_b^{err}}{N_b} \quad (19)$$

where N_b^{err} denotes the total number of erroneous bits and N_b stands for the total number of transmitted bits. As shown from Eq. (18) and Eq. (19), the BER and FER estimates are statistically calculated over a number of transmitted packets in order to obtain their statistical averages at various SNR points. To enhance the reliability of the statistical calculation without performing any redundant computations, an adaptive stopping criterion for simulation is used, which uses FER criteria and a threshold for maximum erroneous frames.

The QC-SC-LDPC codes are evaluated against the conventional DVB-S2X LDPC codes with the same modulation and decoding configurations. The comparative analysis will make it possible to perform a comprehensive study on the coding gains, decoding convergences, error floor performances, and overall error correction improvements achieved by the proposed memory-aware QC-SC-LDPC framework.

3.9 Computational Complexity Analysis

The computational complexity of the proposed QC-SC-LDPC framework stem from three main components which include the pairwise cycle-aware PEG edge-placement process and PEG-based shift optimization and iterative decoding operations. The proposed framework achieves localized graph construction through its cycle-aware optimization feature which results in complexity depending on the number of Tanner graph edges used during protograph generation and quasi-cyclic lifting.

In the case of a protograph that has E graph edges, the pair-wise penalty computation and edge shifting process for the pair-wise cycle aware PEG algorithm would have computational complexity proportional to

$$O(E^2) \qquad (20)$$

As stated by Eq. (20), the complexity of constructing a graph grows quadratically with respect to the number of Tanner graph edges because of repetitive cycle check testing, penalty function computation for pair-wise interactions, and optimal shifting of circulant matrices while constructing edges.

During iterative decoding, the LBP algorithm has the following per iteration computational complexity depending on the number of Tanner graph edges, which can be written as

$$O(E) \qquad (21)$$

The decoding complexity according to Eq. (21) increases with the graph connectivity which enables efficient decoding for long DVB-S2X frame lengths. The quasi-cyclic structure decreases memory requirements because it needs to store only circulant shift indices instead of complete parity-check matrix. The memory-aware banded coupling structure which we developed reduces interconnection complexity while enabling better scalability with high-throughput hardware implementations.

4 Result and Discussion

The section assesses the FER performance of memory-aware QC-SC-LDPC framework testing which was created for DVB-S2X satellite communication systems operating through AWGN channels. The primary objective of this research study examines decoding reliability and convergence characteristics together with SNR improvement which the proposed framework achieves when compared to traditional DVB-S2X LDPC reference codes.

Simulation results based on the short-frame design of DVB-S2X have been obtained through Monte Carlo simulation technique, considering QPSK modulation. LBP decoding has been implemented due to faster convergence behavior and low decoding time latency when compared with conventional flooding-based iterative decoding. The performances of the FERs have been analyzed in terms of both (E_b/N_0) and (E_s/N_0) ratios. The targeted FER for all cases was set at 10^{-5}, which is a commonly recognized measure of reliability in satellite communications.

The QC-SC-LDPC scheme combines deterministic memory-aware spatial coupling, adaptive irregular degree profile, pair-wise cycle-aware PEG edge positioning, and quasi-cyclic shift using PEG. These techniques work together to improve expansion in the Tanner graphs, provide better girth properties, reduce the number of undesirable short cycles, and improve convergence during iterative decoding while retaining the quasi-cyclic property essential for hardware efficiency. Table 2 presents the performance comparison of the proposed QC-SC-LDPC scheme against conventional DVB-S2X LDPC code designs.

Table 2 Performance Comparison of Proposed QC-SC-LDPC and DVB-S2X LDPC Codes

Configuration	**Metric**	**DVB-S2X LDPC**	**Proposed QC-SC-LDPC**	**Coding Gain**
QPSK 32/45 (R=0.7111)	(E_b/N_0) at FER = 10^{-5}	4.88 dB	4.52 dB	0.36 dB
QPSK 11/45 (R = 0.2444)	(E_b/N_0) at FER = 10^{-5}	–2.40 dB	–0.46 dB	2.86 dB
QPSK 11/45 (R=0.2444)	(E_s/N_0) at FER = 10^{-5}	–2.50 dB	–6.75 dB	4.25 dB

For the QPSK 32/45 configuration with code rate R = 0.7111, the FER comparison under E_b/N_0 shows an improvement in terms of FER when comparing to the conventional DVB-S2X LDPC code scheme, as shown in Figure 2. The proposed QC-SC-LDPC framework meets the target FER of 10^{-5} at about 4.52 dB, while the DVB-S2X reference code needs almost 4.88 dB to reach the same level of reliability. This corresponds to a coding gain of approximately 0.36 dB.

Despite the relatively modest quantitative enhancement, this becomes very crucial for the development of efficient satellite communication links at high transmission rates, as any SNR reduction can be converted into additional communication margin, power savings, and reliability gain. In addition, as was noted above, the proposed code demonstrates a faster waterfall-region slope, which points to better performance of iterative decoding algorithms and faster message exchange over the Tanner graph. The reason behind such an improvement is that, due to the use of the banded spatially coupled graph construction and optimal design of the circulant shift distribution, the number of unwanted cycles is decreased and improve graph connectivity. As a result, this framework ensures reliable decoding along with structural regularity conducive to real-life FPGA application.

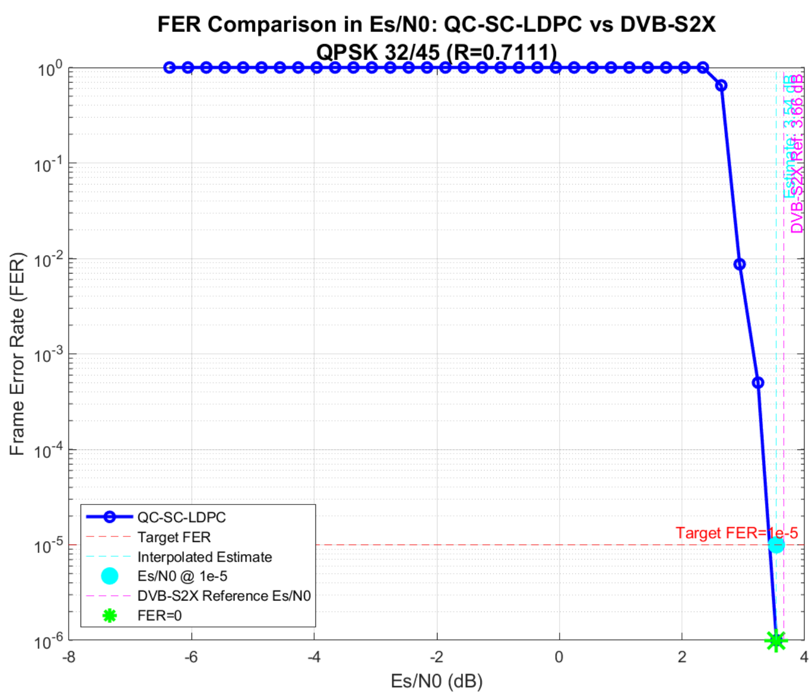

Figure 2 FER comparison of QC-SC-LDPC and DVB-S2X LDPC for QPSK 32/45 over E_b/N_0(R = 0.7111).

The improvement in performance gains is more substantial for the case of the low rate QPSK 11/45 scheme using code rate R = 0.2444, as shown by figures 3-5. The application of low-rate coding techniques is especially crucial in the design of satellite communication systems working under tough channel conditions where stronger error-correction capability is essential.

As can be seen from the FER comparison plot regarding E_s/N_0, as presented in Figure 3, indicates that the proposed QC-SC-LDPC scheme attains the desired FER value around -6.75 dB, while the DVB-S2X baseline code has to be provided with about -2.50 dB for a similar level of performance. The obtained result implies a coding gain greater than 4 dB, which proves the higher stability of the proposed approach under low SNR scenarios.

The decoding efficiency demonstrates consistent properties, in which the proposed QC-SC-LDPC achieves its objective FER value at -6.75 dB, whereas the DVB-S2X standard still maintains its FER value near -2.50 dB, as illustrated in Figure 4. The above consistency confirms the success of the adaptive irregular degree distribution and cycle-aware PEG algorithm in lowering decoding thresholds and improving convergence properties. Moreover, the steepness of the FER curve demonstrates the better expansion properties of the Tanner graph expansion and reduced susceptibility to short, harmful cycles, which are typically responsible for performance degradation in conventional LDPC decoding structures.

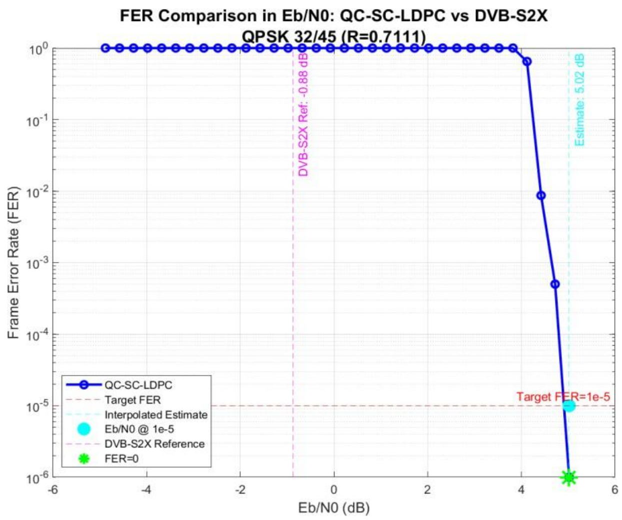

Figure 3 FER comparison of QC-SC-LDPC and DVB-S2X LDPC for QPSK 11/45 over E_s/N_0(R = 0.2444)

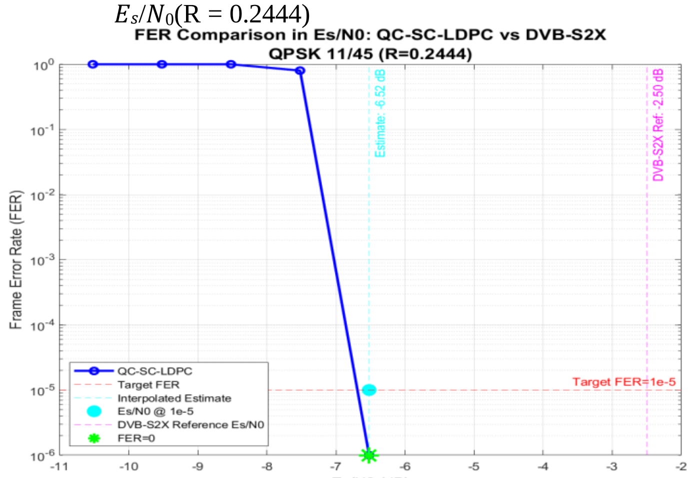

Figure 4 FER performance of QC-SC-LDPC vs DVB-S2X LDPC for QPSK 11/45 over E_s/N_0.

The FER performance under E_b/N_0 for the same QPSK 11/45 configuration, as shown in Figure 5, indicates that the proposed QC-SC-LDPC framework achieves reliable decoding at approximately –0.46 dB, while the DVB-S2X reference code requires around 2.40 dB. The system demonstrates enhanced performance for error correction during times when the signal-to-noise ratio is low. The decoding process shows accelerated performance because the system uses steeper decoding paths which result in faster rate of information transmission through its message-passing system. Such low-SNR decoding capabilities are advantageous for use in advanced satellite communication systems in which energy efficiency, energy saving, and effective long-range data transfer are critical design requirements.

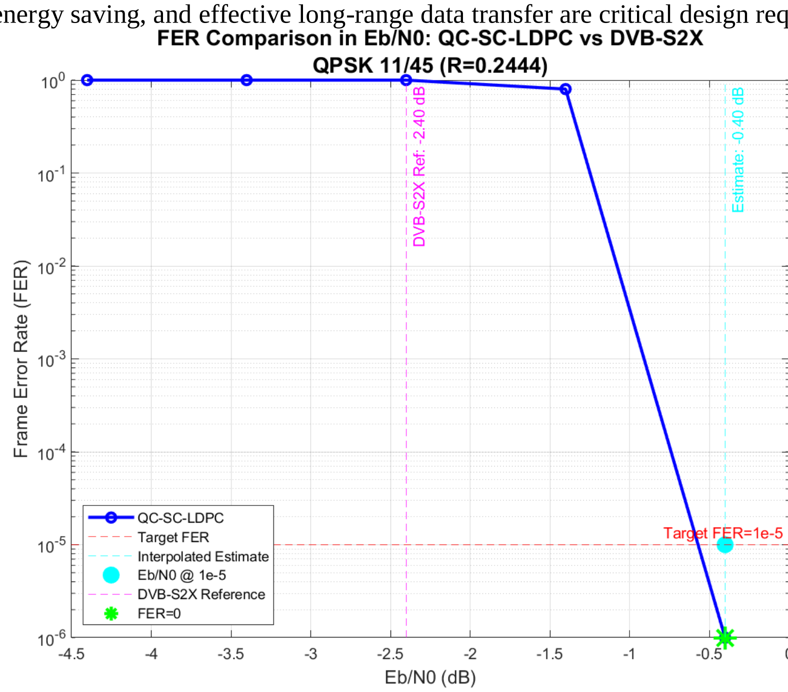

Figure 5 FER comparison of QC-SC-LDPC and DVB-S2X LDPC for QPSK 11/45 over E_b/N_0.

Across all evaluated modulation and coding configurations, the proposed QC-SC-LDPC scheme outperforms the traditional DVB-S2X LDPC benchmark codes based on both their FER and convergence characteristics during decoding. The use of a deterministic memory-based spatial coupling technique is advantageous since it increases local message passing and avoids excessive graph connections, enabling efficient and scalable decoding. Moreover, by employing a quasi-cyclic lifting scheme, there is a significant saving in memory due to storing only the index shifts rather than the entire parity-check matrix. This structural property renders the proposed approach very ideal for high-speed FPGA implementation.

The results of the simulation validate that the proposed scheme has effectively integrated the strengths of both QC-LDPC and SC-LDPC schemes to create a scalable and efficient architecture. The gains in coding performance, the convergence characteristics, and the improved low-SNR decoding performance clearly show that the proposed QC-SC-LDPC scheme is highly suitable for DVB-S2X satellite communication systems in AWGN channels.

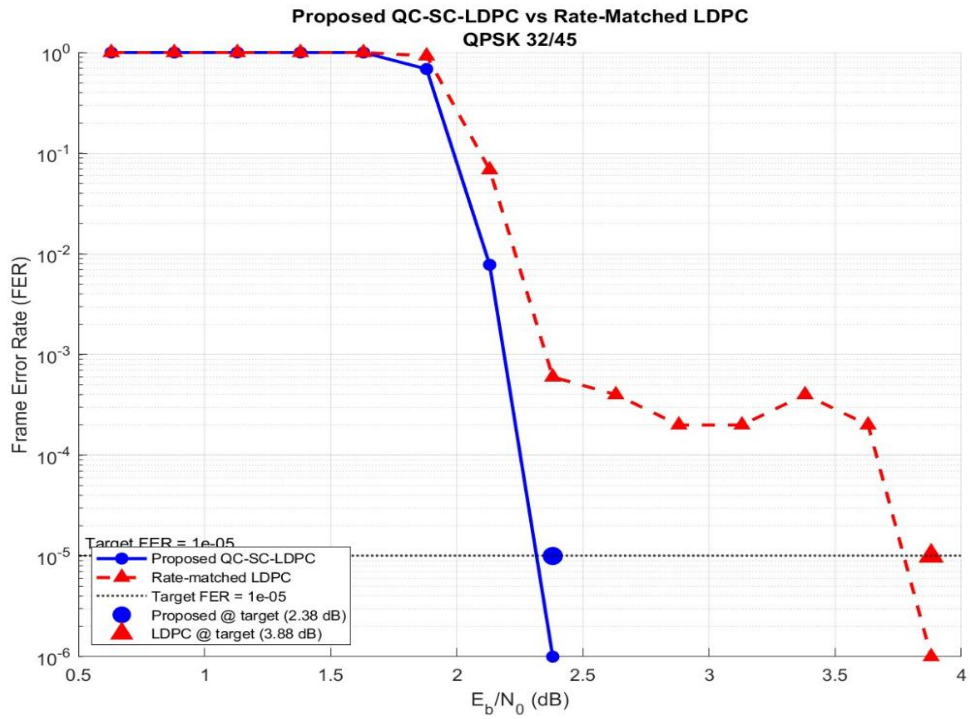

Figure 6 Proposed QC-SC-LDPC vs Rate-Matched LDPC QPSK 32/45

The simulation results demonstrate that the proposed QC-SC-LDPC scheme outperforms the conventional rate-matched LDPC code in terms of frame error rate performance and decoding convergence. The proposed code achieves the target FER at a lower Eb/N_0 value, indicating a significant coding gain and improved reliability under low-SNR conditions.

The superior performance can be attributed to the spatial coupling structure, which enhances message propagation during iterative decoding, while the quasi-cyclic construction ensures implementation efficiency and reduced memory requirements. The observed improvements in error-correction capability and decoding behaviour confirm that the proposed QC-SC-LDPC scheme is a promising solution for DVB-S2X satellite communication systems operating over AWGN channels.

4.1 Discussion

The simulation results show that the proposed memory-aware QC-SC-LDPC framework always works better than traditional DVB-S2X LDPC codes when it comes to FER performance and decoding efficiency over AWGN channels. In the high-rate QPSK 32/45 configuration, the proposed model achieves the target FER at E_b/N_0 = 4.52dB compared to 4.88 dB for the reference, resulting in a coding gain of 0.36 dB. More significant improvements are observed in the low-rate QPSK 11/45 configuration. The proposed system attains the desired FER value of −6.75 dB in E_s/N_0, while it attains the desired FER value of −0.46 dB in E_b/N_0 as opposed to a value of −2.50 dB and 2.40 dB for the reference DVB-S2X, respectively. These results confirm strong robustness under low-SNR conditions.

The improvements in performance can be mostly contributed to the spatial coupling with memory consideration, as it increases the localized message passing efficiency and helps with iterative convergence. Moreover, the irregular degree adaptation contributes to an increase in graph connectivity and decoding thresholds. Lastly, the optimization of the PEG design and quasi-cyclic shifting scheme for short-cycle avoidance helps to improve the Tanner graph properties and decrease decoding errors. In general, the QC-SC-LDPC code structure will result in better performance terms of decoding robustness, fast convergence, and efficiency in implementation due to the above-mentioned advantages over traditional DVB-S2X LDPC codes in satellite communications.

5 Conclusion

This study proposed a QC-SC-LDPC code design framework for reliable DVB-S2X satellite communication systems operating over AWGN channels. The proposed methodology unifies deterministic spatial coupling, adaptive irregular protograph design, pairwise cycle-aware PEG-based construction, and optimized quasi-cyclic lifting within a single structured framework. The integrated design improves Tanner graph connectivity while reducing harmful short cycle and trapping structure instances and enhancing iterative message-passing decoding algorithms. The system improves decoding efficiency through memory-aware banded coupling which creates localized controlled connectivity in the protograph while maintaining regular structural patterns and scalability of the system. Furthermore, the PEG-based optimization method for edgevplacement and circulant shifts delivers better girth performance and enhanced graph expansion capabilities, which essential for achieving dependable satellite channel decoding results. The proposed QC-SC-LDPC framework provides a unified and hardware-efficient coding solution that effectively bridges the gap between structural code design and implementation-oriented requirements in modern DVB-S2X satellite communication systems. The system supports future high-reliability communication needs because its scalable design and enhanced graph characteristics enable better performance. Future extensions may consider adaptation to fading and non-stationary satellite channels, integration with non-terrestrial network (NTN) architectures, and hardware prototyping for real-time deployment.

References

1. K. Guo *et al.*, "Performance analysis of hybrid satellite-terrestrial cooperative networks with relay selection," *IEEE Trans. Veh. Technol.*, vol. 69, no. 8, pp. 9053–9067, 2020.
2. K. Guo, X. Li, M. Alazab, R. H. Jhaveri, and K. An, "Integrated satellite multiple two-way relay networks: Secrecy performance under multiple eves and vehicles with non-ideal hardware," *IEEE Trans. Intell. Veh.*, vol. 8, no. 2, pp. 1307–1318, 2022.
3. G. Sachs, "The global satellite market is forecast to become seven times bigger." [Online]. Available: https://www.goldmansachs.com/insights/articles/the-global-satellite-market-is-forecast-to-become-seven-times-bigger
4. A. Morello and V. Mignone, "DVB-S2: The second generation standard for satellite broad-band services," *Proc. IEEE*, vol. 94, no. 1, pp. 210–227, 2006.
5. M. N. Sweeting, "Modern small satellites-changing the economics of space," *Proc. IEEE*, vol. 106, no. 3, pp. 343–361, 2018.
6. X. Lin *et al.*, "5G new radio evolution meets satellite communications: Opportunities, challenges, and solutions," *5G beyond Fundam. Stand.*, pp. 517–531, 2021.
7. N. Khosroshahi, R. Mankarious, and M. R. Soleymani, "A Novel FEC Implementation for VSAT Terminals Using High-Level Synthesis," *Aerospace*, vol. 13, no. 2, p. 155, 2026.
8. H. Fenech, S. Amos, A. Tomatis, and V. Soumpholphakdy, "High throughput satellite systems: An analytical approach," *IEEE Trans. Aerosp. Electron. Syst.*, vol. 51, no. 1, pp. 192–202, 2015.
9. N. Khosroshahi and T. A. Gulliver, "Quasi-cyclic low density parity check (LDPC) codes for dedicated short range communication (DSRC) systems," in *CCECE 2010*, IEEE, 2010,
10. pp. 1–5.
11. Z. Yang, Y. Fang, G. Zhang, F. C. M. Lau, S. Mumtaz, and D. B. Da Costa, "Analysis and optimization of tail-biting spatially coupled protograph LDPC codes for BICM-ID systems," *IEEE Trans. Veh. Technol.*, vol. 69, no. 1, pp. 390–404, 2019.
12. Q. Wang, S. Cai, W. Lin, S. Zhao, L. Chen, and X. Ma, "Spatially coupled LDPC codes via partial superposition and their application to HARQ," *IEEE Trans. Veh. Technol.*, vol. 70, no. 4, pp. 3493–3504, 2021.
13. T. J. Richardson and R. L. Urbanke, "The capacity of low-density parity-check codes under message-passing decoding," *IEEE Trans. Inf. theory*, vol. 47, no. 2, pp. 599–618, 2001.
14. M. Lentmaier, A. Sridharan, D. J. Costello, and K. S. Zigangirov, "Iterative decoding threshold analysis for LDPC convolutional codes," *IEEE Trans. Inf. Theory*, vol. 56, no. 10,
15. pp. 5274–5289, 2010.
16. S. Kudekar, T. Richardson, and R. L. Urbanke, "Spatially coupled ensembles universally achieve capacity under belief propagation," *IEEE Trans. Inf. Theory*, vol. 59, no. 12, pp. 7761–7813, 2013.
17. R. Tanner, "A recursive approach to low complexity codes," *IEEE Trans. Inf. theory*, vol. 27, no. 5, pp. 533–547, 1981.
18. L. Dolecek, Z. Zhang, V. Anantharam, M. J. Wainwright, and B. Nikolic, "Analysis of absorbing sets and fully absorbing sets of array-based LDPC codes," *IEEE Trans. Inf. Theory*, vol. 56, no. 1, pp. 181–201, 2009.
19. M. Karimi and A. H. Banihashemi, "On characterization of elementary trapping sets of variable-regular LDPC codes," *IEEE Trans. Inf. theory*, vol. 60, no. 9, pp. 5188–5203, 2014.
20. X. Tao, Y. Li, Y. Liu, and Z. Hu, "On the construction of LDPC codes free of small trapping sets by controlling cycles," *IEEE Commun. Lett.*, vol. 22, no. 1, pp. 9–12, 2017.
21. D. J. C. MacKay, "Good error-correcting codes based on very sparse matrices," *IEEE Trans. Inf. Theory*, vol. 45, no. 2, pp. 399–431, 2002.

22. M. P. C. Fossorier, M. Mihaljevic, and H. Imai, "Reduced complexity iterative decoding of low-density parity check codes based on belief propagation," *IEEE Trans. Commun.*, vol. 47, no. 5, pp. 673–680, 1999.
23. N. Wiberg, H. Loeliger, and R. Kotter, "Codes and iterative decoding on general graphs," *Eur. Trans. Telecommun.*, vol. 6, no. 5, pp. 513–525, 1995.
24. D. V. Nguyen, S. K. Chilappagari, M. W. Marcellin, and B. Vasic, "On the construction of structured LDPC codes free of small trapping sets," *IEEE Trans. Inf. Theory*, vol. 58, no. 4,
25. pp. 2280–2302, 2012.

26. J. Kang, Q. Huang, S. Lin, and K. Abdel-Ghaffar, "An iterative decoding algorithm with backtracking to lower the error-floors of LDPC codes," *IEEE Trans. Commun.*, vol. 59, no. 1, pp. 64–73, 2010.
27. D. G. M. Mitchell, M. Lentmaier, and D. J. Costello, "Spatially coupled LDPC codes constructed from protographs," *IEEE Trans. Inf. Theory*, vol. 61, no. 9, pp. 4866–4889, 2015.
28. Y. Zhang, K. Peng, J. Song, and Y. Wu, "Quasi-cyclic spatially coupled LDPC code for broadcasting," *IEEE Trans. Broadcast.*, vol. 66, no. 1, pp. 187–194, 2019.
29. Z. He, K. Peng, J. Song, and Y. Zhang, "Sliding window decoding for QC-SC-LDPC codes under the constraint of implementation complexity," *IEEE Trans. Broadcast.*, vol. 68, no. 2, pp. 305–316, 2022.
30. F. Steiner, E. Ben Yacoub, B. Matuz, G. Liva, and A. G. i Amat, "One and two bit message passing for SC-LDPC codes with higher-order modulation," *J. Light. Technol.*, vol. 37, no. 23, pp. 5914–5925, 2019.
31. M. Battaglioni, A. Tasdighi, G. Cancellieri, F. Chiaraluce, and M. Baldi, "Design and
32. analysis of time-invariant SC-LDPC convolutional codes with small constraint length," *IEEE Trans. Commun.*, vol. 66, no. 3, pp. 918–931, 2017.
33. M. Battaglioni, F. Chiaraluce, M. Baldi, and M. Lentmaier, "Girth analysis and design of periodically time-varying SC-LDPC codes," *IEEE Trans. Inf. Theory*, vol. 67, no. 4, pp. 2217–2235, 2021.
34. D. J. C. MacKay and R. M. Neal, "Near Shannon limit performance of low density parity check codes," *Electron. Lett.*, vol. 32, no. 18, pp. 1645–1646, 1996.
35. R. Chauvat, A. Garcia-Pena, and M. Paonni, "Efficient LDPC-coded CCSK links for robust high data rates GNSS," *IEEE Trans. Aerosp. Electron. Syst.*, vol. 59, no. 1, pp. 404–417, 2022.
36. Y. Fang, G. Bi, Y. L. Guan, and F. C. M. Lau, "A survey on protograph LDPC codes and their applications," *IEEE Commun. Surv. Tutorials*, vol. 17, no. 4, pp. 1989–2016, 2015.
37. L. Song, S. Yu, and Q. Huang, "Low-density parity-check codes: Highway to channel capacity," *China Commun.*, vol. 20, no. 2, pp. 235–256, 2023.
38. C. Zhang, X. Mu, J. Yuan, H. Li, and B. Bai, "Construction of multi-rate quasi-cyclic LDPC codes for satellite communications," *IEEE Trans. Commun.*, vol. 69, no. 11, pp. 7154–7166, 2021.
39. G. Li, I. J. Fair, and W. A. Krzymien, "Density evolution for nonbinary LDPC codes under Gaussian approximation," *IEEE Trans. Inf. Theory*, vol. 55, no. 3, pp. 997–1015, 2009.
40. Y. Koizumi, Y. Suzuki, T. Kusunoki, K. Yokohata, and H. Sujikai, "Study on error correction in IP network with LDPC codes for satellite broadcasting and coding rate conversion method with padding bits," in *2020 10th Advanced Satellite Multimedia Systems Conference and the 16th Signal Processing for Space Communications Workshop (ASMS/SPSC)*, IEEE, 2020, pp. 1–6.
41. O. Vassallo, V. Buttigieg, and M. A. Azzopardi, "An Energy Efficient Hybrid FEC-ARQ Communication Scheme for Small Satellite Applications," in *2021 International Conference on Computer, Information and Telecommunication Systems (CITS)*, IEEE, 2021, pp. 1–6.
42. B. Gumede, E. Mukubwa, N. Pillay, and I. E. Davidson, *Performance Analysis of Filtered Orthogonal Frequency Division Multiplexed LDPC Codes for Satellite Communication in the Ka-Band*. IEEE, 2023.
43. L. Li, X. Yao, Y. Li, R. Zhu, J. Lv, and H. Li, "Resource-efficient and ultra-high throughput LDPC decoder for CCSDS near-earth standard," *Integration*, vol. 103, p. 102390, 2025.
44. Y. Xu, M. Jiang, M. Zhu, N. Hu, C. Zhao, and J. Wang, "Reduced-complexity decoding of 3D product codes for satellite communications," *Sp. Sci. Technol.*, vol. 4, p. 96, 2024.
45. H. KANG, M. JIANG, and Q. WANG, "Spatially coupled LDPC codes based on multi-weight circulant matrix decomposition," *J. Tsinghua Univ. (Science Technol.*, vol. 65, no. 11, pp. 2024–2031, 2025.
46. Y. He and Y. Wang, "Research on low-density parity-check decoding algorithm for reliable transmission in satellite communications," *Appl. Sci.*, vol. 14, no. 2, p. 746, 2024.
47. Y. Li, Y. Li, N. Ye, T. Chen, Z. Wang, and J. Zhang, "High throughput priority-based layered QC-LDPC decoder with double update queues for mitigating pipeline conflicts," *Sensors*, vol. 22, no. 9, p. 3508, 2022.
48. W. Khawaja, N. J. H. Marcano, and R. H. Jacobsen, "Improvement of DVB-S2/S2X Performance Using External Synchronization," *arXiv Prepr. arXiv2604.07358*, 2026.